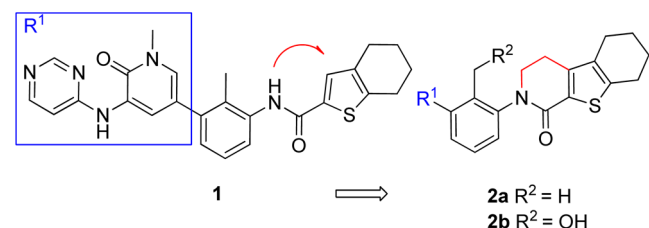


Table 1. Improved Properties of Tricyclic H3 Btk Inhibitors



ID	IC ₅₀ (μM) ^a				Rat	
	Btk	CD86	LLE ^b	hPPB ^c	CL ^d	F% ^e
1	0.042	0.74	3.6	99%	2	45%
2a	0.011		4.2	99%		
2b	0.001	0.087	5.8	97%	2	90%

^aAssay protocols in Supporting Information (SI), $n \geq 2$. ^bLLE = $\text{pIC}_{50}(\text{Btk}) - \text{cgLogD}$. ^cHuman plasma protein binding. ^dTotal clearance (mL/min/kg) at 1 mg/kg i.v. dose formulated using a mixture of EtOH/Cremophor/water for **1** (solution) or PEG400/EtOH/water for **2b** (solutions). ^eF% = oral bioavailability after a 5 mg/kg oral dose ($n = 3$) formulated using a mixture of EtOH and Cremophor for **1** (solution) or PEG400/EtOH/Tween80/water for **2b** (suspension).

compound **1**. With the improved potency and/or decreasing lipophilicity, the lipophilic ligand efficiency (LLE) increased sequentially from **1** (3.6) to **2a** (4.2) to **2b** (5.8), indicating enhanced druglike properties. The cellular potency of compound **2b** (IC₅₀ = 0.087 μM), as measured by inhibition of CD86 surface expression on B cells, is 8-fold higher than that of **1** (IC₅₀ = 0.74 μM). Additionally, **2b** is 2-fold more orally bioavailable (90%) than **1** (45%) and has similarly low clearance in rat.

Modeling of **1** and **2b** in the Btk catalytic domain is shown in Figure 1. The tricyclic system did not alter the overall predicted

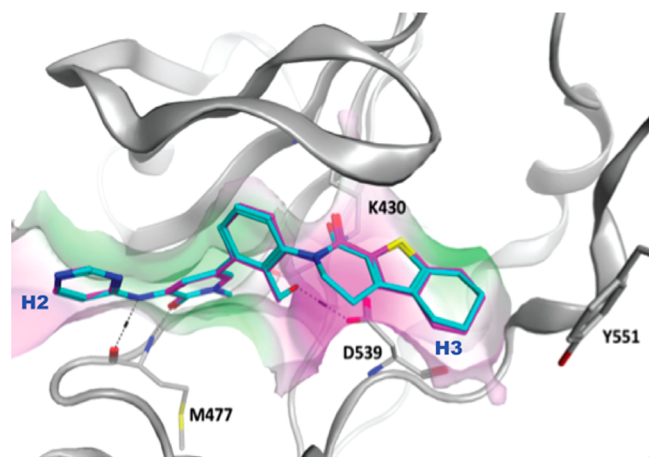


Figure 1. Superposition of modeled structures of **1** (magenta) and **2b** (cyan) in the Btk catalytic domain. H-bonds to the protein are shown as black cylinders with dashed lines. The active site surface is shown color coded by lipophilicity (green, nonpolar; purple, polar).

ligand binding mode, and preserved the interactions at the kinase selectivity H3 pocket with the neighboring hydrophobic residues. Specific interactions with Y551 and K430 were maintained. The hydroxymethyl on the central benzene ring projected into a water-filled cavity, and formed H-bonds with K430 and D539.

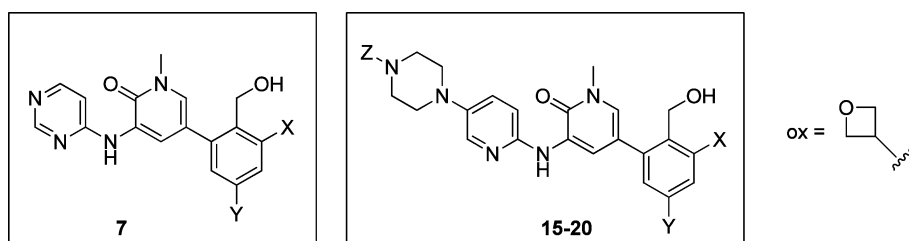
The success of our initial attempts at creating improved Btk inhibitors by the employment of a tricyclic moiety encouraged us to explore additional tricycles at this position as well as carefully designed bicycles. Table 2 shows a selected subset of such compounds. Compounds **2b–6** are examples of inhibitors that contain distal 6–5–6 tricyclic ring systems. Since the H3 site is lipophilic, with nonpolar residues flanking much of this pocket, it is not surprising that the most potent compounds, **2b** and **3** (Btk IC₅₀ = 0.001 and 0.006 μM respectively), contain all-carbon fused cyclohexane rings.

Table 2. SAR for H3 Groups

ID	R	IC ₅₀ (μM) ^a		Sol. (μM) ^b
		Btk	CD86	
2b		0.001	0.087	2
3		0.006	0.2	49
4		0.081	0.48	85
5		2.6	48.6	36
6		16.7	>50	124
7		0.002	0.064	1.4
G-744		0.002	0.057	1
8		0.002	0.057	1
9		-	0.051	2
10		0.003	0.193	2
11		0.139	NT	56
12		0.003	1.2	8
13		0.004	0.171	15
14		0.005	0.23	2

^aAssay protocol in SI, $n \geq 2$. ^bKinetic solubility was measured at pH 7.4.¹⁷

Table 3. Combination of the Best H2 and H3 Moieties for Optimal Potency and Druglike Properties



ID	X	Y	Z	IC ₅₀ (μM) ^a			HHep/ RHep ^b	Sol. (μM) ^c	Perm. ^d	Rat	
				Btk	CD86	WB CD69				CL ^e	F% ^f
7		H	n/a	0.002	0.064	0.087	11 / <10	1.4	MOD	16	41
15		H	Me	0.003	0.025	-	<6.2 / <10	18	-	29	37
16		H	ox	0.004	0.006	0.089	8.8 / <10	1	MOD	-	-
17		H	Me	0.004	0.107	0.045	10 / 12	115	MOD	40	20
18		H	ox	0.008	0.137	0.069	<6 / <10	99	MOD	14	46
19		F	Me	0.002	0.022	0.029	<6.2 / <10.1	71	MOD	37	52
20		F	ox	0.004	0.010	0.035	<6 / <10	73	HIGH	20	27

^a Assay protocol in SI, $n \geq 2$. ^b Projected hepatic clearance using human or rat hepatocytes. ^c Kinetic solubility was measured at pH 7.4. ^d Measured permeability using Madin-Darby Canine Kidney (MDCK) Epithelial cell lines, A to B; MOD: 1–10 (10^{-6} cm/s) and HIGH: >10 (10^{-6} cm/s). ^e Total clearance (mL/min/kg) at 1 mg/kg i.v. dose formulated using a mixture of PEG400/ethanol/water for 7, 15, and 17–20 (solution). ^f F% = oral bioavailability after 5 mg/kg oral dose ($n = 3$) formulated using a mixture of PEG400/ethanol/Tween80/water for 7 (suspension), PEG400/ethanol/water for 17 (suspension), 15, 18–20 (solution).

Compound 4, with a heteroatom in the right-hand saturated ring, displayed reduced potency (Btk IC₅₀ = 0.081 μM), while 5 and 6 were much less potent, presumably due to the reduced lipophilicity of the tricycle. Modeling indicated that there was an opportunity to further flesh out the H3 pocket and that gem dimethyl substituted 6–5–5 systems might offer some advantages by occupying more of the lipophilic H3 pocket. The resulting 6–5–5 compounds 7 and 8 of 2b and 3, respectively, were equipotent to slightly more potent against Btk (IC₅₀ = 0.002 μM), and both had improved cell potencies.

We also examined bicyclic 6–6 fused (9), 5–5 fused (10–11), and 5–6 fused (12) ring systems containing appropriately placed *tert*-butyl groups to extend into the H3 pocket. Among this group, the 5–5, 5–6 fused 10 and 12 had the highest enzyme binding potency (Btk IC₅₀'s = 0.003 μM) but were relatively less potent in the CD86 cellular assay.

Finally, we surveyed 7–6 ring systems (13 and 14). These compounds were less appealing due to their decreased biochemical and cell potencies. The cell potencies of all compounds mostly tracked with biochemical potencies, with the Btk/CD86 IC₅₀ ratio ranging from 6- (4) to 64- (10) fold. The only major outlier was the bicyclic compound 12, which had a cell shift of 400-fold. Presumably, this shift was due to differences in plasma protein binding and cell permeability of this compound. Other researchers have reported on a variety of bicyclic H3 moieties within alternate series;^{18–20} however, we are the first group to describe highly potent and Btk-selective tricyclic 6–5–6 and 6–5–5 compounds.

With a variety of novel tricyclic compounds in hand that had excellent potency for Btk, we focused our efforts on designing compounds with improved physicochemical properties. As demonstrated in Table 2, although compounds 2b, 7, 8, and 9 had the best cellular potency (CD86 IC₅₀ < 100 nM), they unfortunately all had low kinetic solubility (<2 μM) at physiological pH. Kinetic solubility as measured in an internal high throughput assay¹⁷ was used as an initial gauge of intrinsic solubility. Low solubility is a primary cause of reduced oral bioavailability of the crystalline materials preferred for clinical development, and often presents formulation challenges in dose escalations for safety studies. This was indeed the case for many compounds in this chemical series. To find compounds with improved solubility, modifications of the left-hand portion of the inhibitor that extends into a partially solvent exposed area of the protein region ("H2", Figure 1) were explored and found to be well tolerated. Of the many compounds generated,²¹ we determined that compounds with a substituted pyridinopiperazine group (Table 3), as opposed to the pyrimidine of the previous compounds (Table 2), offered an exciting new subseries with much improved kinetic solubility.

A small subset of compounds containing combinations of the best H2 and H3 groups are highlighted in Table 3. Installing a tertiary basic amine containing left-hand H2, which is primarily protonated at neutral pH, indeed helped improve the solubility from 1.4 μM (7) to 18 μM (15). Reducing the basicity from a calculated pK_a of 7.8 (15) to 6.3 (16, substituted with an oxetane)²² abrogated the improved solubility. This prompted

us to focus on H3 groups with higher polarity than that of 7. Gratifyingly, all four compounds containing a more polar tetrahydroindole H3 group (17–20) maintained high kinetic solubility regardless of the amine basicity. However, the moderate CD86 cellular potencies of 17 and 18 (IC_{50} 's of 0.107 and 0.137 μ M, respectively) mirrored that of the 0.2 μ M potency seen for 3, which bears the same polar H3 group. A potency breakthrough was realized when a single fluorine atom was added to the middle linker benzene ring (19–20). This fluorine is well positioned to engage the backbone carbonyl carbon of G409 in a dipole–dipole interaction (Figure s1 in the SI), further stabilizing the binding orientation of these inhibitors in the Btk catalytic domain. The resultant CD86 cellular potency improved 5-fold and 13-fold for the two pairs 17 \rightarrow 19 and 18 \rightarrow 20, respectively.

All compounds in Table 3, except 17, were low to moderately cleared and had reasonable bioavailability in *in vivo* rat PK studies. *In vitro* hepatic clearance represented by RHEP data underestimated the *in vivo* clearance; however, the relative stability trend was consistent from *in vitro* to *in vivo* studies. It was also pleasing to see that human hepatic clearance ranged from low to moderate. Given the totality of data including safety assessment (not discussed here), compounds 7 (G-744) and 20 rose to the top of the list with the most balanced overall profile.

In addition to potency and druglike properties, a prominent goal of developing a clinically viable kinase inhibitor lies in controlling selectivity. Poor selectivity may have a profound effect on drug safety, especially for nononcology indications where chronic dosing requires an exquisitely clean safety profile. Therefore, both G-744 and 20 were profiled against a panel of 285 active recombinant human kinases. In particular, G-744 demonstrated >1000-fold Btk biochemical selectivity against all kinases tested except for EphA7 and Fgr, against which it still showed robust selectivity of 428-fold and 868-fold, respectively (Figure s3 in the SI). Due to G-744's superb kinase selectivity (superior to 20), we realized it could be an excellent tool molecule to probe the biology of Btk, as the results would not be confounded by off-target activity and the need for interpretation. Thus, we performed a full characterization of this molecule, with key data summarized in Table 4. In addition

Table 4. Additional G-744 Potency Data (mean \pm SEM)

Assay	$K_{i,app}$ or EC_{50} (nM)
Btk biochemical, ($K_{i,app}$)	1.28 \pm 0.13 [$n = 3$]
Mouse splenocyte B cell CD86	55 and 75 [$n = 2$]
Human Whole Blood B cell CD69	87 \pm 30 [$n = 11$]
Human B cell proliferation	22 \pm 3 [$n = 17$]
Human monocyte TNF α production	33 \pm 6 [$n = 12$]

to preventing cellular functions in murine B-cells such as B-cell receptor (BCR)-mediated CD86 induction with an EC_{50} of 64 nM, G-744 also inhibited BCR-stimulated B-cell proliferation in human B-cells ($EC_{50} = 22$ nM). In human monocytes, production of the inflammatory cytokine TNF α following activation with immune complexes was abrogated by G-744 ($EC_{50} = 33$ nM). In human whole blood, G-744 demonstrated potent inhibition of BCR-stimulated CD69 expression on B-cells with an EC_{50} of 87 nM.

In pharmacokinetic experiments, G-744 exhibited low to moderate clearance in four preclinical species (Table 5). Sufficient oral exposures were achievable using a crystalline

formulation in both mouse and rat despite low kinetic solubility.

Table 5. Preclinical DMPK Profiling of G-744

Species	In vitro		In vivo	
	LM CL_{hep}^a	Hep CL_{hep}^b	CL ^c	F% ^d
mouse	35	2	22	45 ^e – 77 ^f
rat	18	3	16	23 ^e – 37 ^f
dog	15	1	7	27 ^f
cyno	18	31	17	
human	8	11		

^aProjected hepatic clearance using liver microsomes (mL/min/kg). ^bProjected hepatic clearance using hepatocytes (mL/min/kg). ^cTotal clearance *in vivo* (mL/min/kg). ^dF% = oral bioavailability after 5 (amorphous) or 100 mg/kg (crystalline) dose in mouse; 5 (amorphous) or 100 mg/kg (crystalline) dose in rat; 5 mg/kg dose in dog ($n = 3$). ^eMethylcellulose/Tween80/water suspension of crystalline free base material. ^fHydroxypropylmethylcellulose/Na citrate/water pH 3 suspension of amorphous material.

Given the favorable DMPK profile of G-744 in rat, we examined its efficacy in the developing collagen-induced arthritis (CIA) model in Lewis rat.^{3,23} Oral dosing with G-744 at 6.25, 12.5, and 25 mg/kg b.i.d. maintained plasma concentrations above the IC_{50} , IC_{70} , and IC_{90} , respectively, for inhibition of Btk Y223 phosphorylation in whole blood (Figure s2 in the SI). As shown in Figure 2, all three doses resulted in a

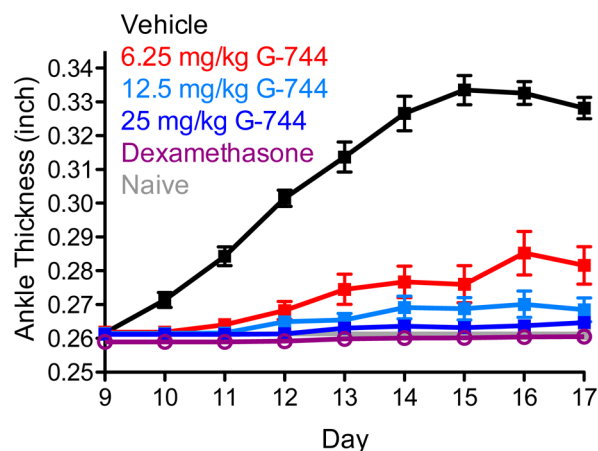


Figure 2. Results from a CIA study in rats. Treatment with G-744 protects Lewis rats from collagen-induced arthritis. Female Lewis rats ($n = 10$ per group) with developing CIA were dosed orally with G-744 as indicated (b.i.d.) or with 0.05 mg/kg dexamethasone daily starting on day 0. Daily ankle diameter measurements are shown as mean \pm SEM and were significantly (by ANOVA) reduced toward normal for all drug-treated rats (significant days 10–17) as compared to the vehicle control.

significant dose-dependent inhibition of ankle thickness between day 10 and day 17 (onset of increase in ankle diameter on day 9). The 25 mg/kg dose (97% inhibition of the area under the ankle thickness vehicle curve) showed comparable efficacy to dexamethasone. In naïve rats treated with vehicle, the ankle diameters did not change over the course of the study and ankles from normal rats were significantly different ($P < 0.05$) compared with the CIA rats treated with vehicle. In addition, G-744 was also highly efficacious in preventing Interferon α -driven lupus nephritis.²⁴

In summary, orally bioavailable Btk inhibitors with novel tricyclic head groups were discovered through structure and property based drug design. Improved molecules were discovered, and an outstanding tool molecule, G-744, was identified with excellent potency, favorable DMPK properties, and superb kinase selectivity. G-744 demonstrated efficacy equivalent to Dexamethasone in a rat CIA model at 25 mg/kg b.i.d. dosing. Such findings further solidified our commitment to Btk as a therapeutic target. The chemistry culminating in a clinical candidate will be described in a subsequent manuscript.

■ ASSOCIATED CONTENT

Supporting Information

The Supporting Information is available free of charge on the ACS Publications website at DOI: 10.1021/acsmchemlett.7b00103.

Physicochemical properties, experimental procedures, compound characterization, assay protocols, PK–PD relationship, and full kinome data (PDF)

■ AUTHOR INFORMATION

Corresponding Authors

*E-mail: wang.xiaojing@gene.com (X. Wang).

*E-mail: young.wendy@gene.com (W. B. Young).

ORCID

Xiaojing Wang: 0000-0003-1575-3227

Joseph W. Lubach: 0000-0002-5806-0204

Funding

Thanks to Genentech, a member of the Roche Group for the research funds.

Notes

The authors declare no competing financial interest.

Biographies

Xiaojing Wang received a B.S. degree from Peking University, a Ph.D. in Organic Chemistry from University of Florida under the supervision of Kenan Professor Alan R. Katritzky, and was a Postdoctoral Fellow at RTI International with Dr. C. Edgar Cook. Since then, Xiaojing has pursued drug discovery of various disease indications at ISIS (now Ionis), Scios/Johnson and Johnson, and Genentech/Roche. Xiaojing is currently a Senior Scientist of Discovery Chemistry at Genentech and has led multidisciplinary teams into nominating several clinical candidates as a project team lead. Xiaojing is an inventor and author of over 40 patents and research publications.

Wendy B. Young received a B.A./M.S. in chemistry from WFU under the guidance of Huw Davies, a Ph.D. from Princeton University under the direction of E. C. Taylor, and was a Postdoctoral Fellow at Sloan-Kettering in the laboratory of Samuel Danishefsky. Since then, Wendy has led drug discovery efforts at both small biotech firms (Axys/Celera) and larger pharma companies (Genentech/Roche). Wendy is currently Vice President of Discovery Chemistry at Genentech where her teams have produced numerous drug candidates in multiple disease indications. She is listed as an inventor or author on over 70 patents and research publications. Wendy is currently the 2017 elected Chair of the ACS MEDI division.

■ ACKNOWLEDGMENTS

We are grateful to analytical, purification chemistry and compound management group for compound characterization, purification, and handling.

■ ABBREVIATIONS

Btk, Bruton's tyrosine kinase; RA, Rheumatoid arthritis; SLE, systemic lupus erythematosus; MS, multiple sclerosis; MCL, mantle cell lymphoma; CLL, chronic lymphocytic leukemia; BCR, B-cell receptor; DMPK, drug metabolism and pharmacokinetics; CIA, collagen-induced arthritis; b.i.d., twice a day; SEM, standard error of the mean

■ REFERENCES

- (1) Satterthwaite, A. B.; Witte, O. N. The Role of Bruton's Tyrosine Kinase in B-Cell Development and Function: a Genetic Perspective. *Immunol. Rev.* **2000**, *175*, 120–127.
- (2) Brunner, C.; Müller, B.; Wirth, T. Bruton's Tyrosine Kinase Is Involved in Innate and Adaptive Immunity. *Histol. Histopathol.* **2005**, *20* (3), 945–955.
- (3) Di Paolo, J. A.; Huang, T.; Balazs, M.; Barbosa, J.; Barck, K. H.; Bravo, B. J.; Carano, R. A. D.; Darrow, J.; Davies, D. R.; DeForge, L. E.; Diehl, L.; Ferrando, R.; Gallion, S. L.; Giannetti, A. M.; Gribling, P.; Hurez, V.; Hymowitz, S. G.; Jones, R.; Kropf, J. E.; Lee, W. P.; Maciejewski, P. M.; Mitchell, S. A.; Rong, H.; Staker, B. L.; Whitney, J. A.; Yeh, S.; Young, W. B.; Yu, C.; Zhang, J.; Reif, K.; Currie, K. S. Specific Btk Inhibition Suppresses B Cell- and Myeloid Cell-Mediated Arthritis. *Nat. Chem. Biol.* **2011**, *7* (1), 41–50.
- (4) Puri, K. D.; Di Paolo, J. A.; Gold, M. R. B-Cell Receptor Signaling Inhibitors for Treatment of Autoimmune Inflammatory Diseases and B-Cell Malignancies. *Int. Rev. Immunol.* **2013**, *32* (4), 397–427.
- (5) Robak, T.; Robak, E. Tyrosine Kinase Inhibitors as Potential Drugs for B-Cell Lymphoid Malignancies and Autoimmune Disorders. *Expert Opin. Invest. Drugs* **2012**, *21* (7), 921–947.
- (6) Lou, Y.; Owens, T. D.; Kuglstatler, A.; Kondru, R. K.; Goldstein, D. M. Bruton's Tyrosine Kinase Inhibitors: Approaches to Potent and Selective Inhibition, Preclinical and Clinical Evaluation for Inflammatory Diseases and B Cell Malignancies. *J. Med. Chem.* **2012**, *55* (10), 4539–4550.
- (7) Currie, K. S. In *2015 Medicinal Chemistry Reviews*; Desai, M. C., Ed.; ACS Division of Medicinal Chemistry: Washington, DC, 2016; pp 225–234.
- (8) Xing, L.; Huang, A. Bruton's TK Inhibitors: Structural Insights and Evolution of Clinical Candidates. *Future Med. Chem.* **2014**, *6* (6), 675–695.
- (9) Young, W. B.; Barbosa, J.; Blomgren, P.; Bremer, M. C.; Crawford, J. J.; Dambach, D.; Eigenbrot, C.; Gallion, S.; Johnson, A. R.; Kropf, J. E.; Lee, S. H.; Liu, L.; Lubach, J. W.; Macaluso, J.; Maciejewski, P.; Mitchell, S. A.; Ortwine, D. F.; Di Paolo, J.; Reif, K.; Scheerens, H.; Schmitt, A.; Wang, X.; Wong, H.; Xiong, J.-M.; Xu, J.; Yu, C.; Zhao, Z.; Currie, K. S. Discovery of Highly Potent and Selective Bruton's Tyrosine Kinase Inhibitors: Pyridazinone Analogs with Improved Metabolic Stability. *Bioorg. Med. Chem. Lett.* **2016**, *26* (2), 575–579.
- (10) Young, W. B.; Barbosa, J.; Blomgren, P.; Bremer, M. C.; Crawford, J. J.; Dambach, D.; Gallion, S.; Hymowitz, S. G.; Kropf, J. E.; Lee, S. H.; Liu, L.; Lubach, J. W.; Macaluso, J.; Maciejewski, P.; Maurer, B.; Mitchell, S. A.; Ortwine, D. F.; Di Paolo, J.; Reif, K.; Scheerens, H.; Schmitt, A.; Sowell, C. G.; Wang, X.; Wong, H.; Xiong, J.-M.; Xu, J.; Zhao, Z.; Currie, K. S. Potent and Selective Bruton's Tyrosine Kinase Inhibitors: Discovery of GDC-0834. *Bioorg. Med. Chem. Lett.* **2015**, *25* (6), 1333–1337.
- (11) Johnson, A. R.; Kohli, P. B.; Katewa, A.; Gogol, E.; Belmont, L. D.; Choy, R.; Penuel, E.; Burton, L.; Eigenbrot, C.; Yu, C.; Ortwine, D. F.; Bowman, K.; Franke, Y.; Tam, C.; Estevez, A.; Mortara, K.; Wu, J.; Li, H.; Lin, M.; Bergeron, P.; Crawford, J. J.; Young, W. B. Battling Btk Mutants with Noncovalent Inhibitors That Overcome Cys481 and Thr474 Mutations. *ACS Chem. Biol.* **2016**, *11* (10), 2897–2907.
- (12) Watterson, S. H.; De Lucca, G. V.; Shi, Q.; Langevine, C. M.; Liu, Q.; Batt, D. G.; Beaudoin Bertrand, M.; Gong, H.; Dai, J.; Yip, S.; Li, P.; Sun, D.; Wu, D.-R.; Wang, C.; Zhang, Y.; Traeger, S. C.; Pattoli, M. A.; Skala, S.; Cheng, L.; Obermeier, M. T.; Vickery, R.; Discenza, L. N.; D'Arienzo, C. J.; Zhang, Y.; Heimrich, E.; Gillooly, K. M.; Taylor,

T. L.; Pulicicchio, C.; McIntyre, K. W.; Galella, M. A.; Tebben, A. J.; Muckelbauer, J. K.; Chang, C.; Rampulla, R.; Mathur, A.; Salter-Cid, L.; Barrish, J. C.; Carter, P. H.; Fura, A.; Burke, J. R.; Tino, J. A. Discovery of 6-Fluoro-5-(R)-(3-(S)-(8-Fluoro-1-Methyl-2,4-Dioxo-1,2-Dihydroquinazolin-3(4H)-Yl)-2-Methylphenyl)-2-(S)-(2-Hydroxypropan-2-Yl)-2,3,4,9-Tetrahydro-1H-Carbazole-8-Carboxamide (BMS-986142): a Reversible Inhibitor of Bruton's Tyrosine Kinase (BTK) Conformationally Constrained by Two Locked Atropisomers. *J. Med. Chem.* **2016**, *59* (19), 9173–9200.

(13) Liu, J.; Guiadeen, D.; Krikorian, A.; Gao, X.; Wang, J.; Boga, S. B.; Alhassan, A.-B.; Yu, Y.; Vaccaro, H.; Liu, S.; Yang, C.; Wu, H.; Cooper, A.; de Man, J.; Kaptein, A.; Maloney, K.; Hornak, V.; Gao, Y.-D.; Fischmann, T. O.; Raaijmakers, H.; Vu-Pham, D.; Presland, J.; Mansueto, M.; Xu, Z.; Leccese, E.; Zhang-Hoover, J.; Knemeyer, I.; Garlisi, C. G.; Bays, N.; Stivers, P.; Brandish, P. E.; Hicks, A.; Kim, R.; Kozlowski, J. A. Discovery of 8-Amino-Imidazo[1,5-*a*]Pyrazines as Reversible BTK Inhibitors for the Treatment of Rheumatoid Arthritis. *ACS Med. Chem. Lett.* **2016**, *7* (2), 198–203.

(14) De Lucca, G. V.; Shi, Q.; Liu, Q.; Batt, D. G.; Beaudoin Bertrand, M.; Rampulla, R.; Mathur, A.; Discenza, L.; D'Arienzo, C.; Dai, J.; Obermeier, M.; Vickery, R.; Zhang, Y.; Yang, Z.; Marathe, P.; Tebben, A. J.; Muckelbauer, J. K.; Chang, C. J.; Zhang, H.; Gillooly, K.; Taylor, T.; Pattoli, M. A.; Skala, S.; Kukral, D. W.; McIntyre, K. W.; Salter-Cid, L.; Fura, A.; Burke, J. R.; Barrish, J. C.; Carter, P. H.; Tino, J. A. Small Molecule Reversible Inhibitors of Bruton's Tyrosine Kinase (BTK): Structure-Activity Relationships Leading to the Identification of 7-(2-Hydroxypropan-2-Yl)-4-[2-Methyl-3-(4-Oxo-3,4-Dihydroquinazolin-3-Yl)Phenyl]-9H-Carbazole-1-Carboxamide (BMS-935177). *J. Med. Chem.* **2016**, *59* (17), 7915–7935.

(15) Gayko, U.; Fung, M.; Clow, F.; Sun, S.; Faust, E.; Price, S.; James, D.; Doyle, M.; Bari, S.; Zhuang, S. H. Development of the Bruton's Tyrosine Kinase Inhibitor Ibrutinib for B Cell Malignancies. *Ann. N. Y. Acad. Sci.* **2015**, *1358* (1), 82–94.

(16) Blomgren, P. A.; Lee, S. H.; Mitchell, S. A.; Xu, J.; Schmitt, A. C.; Kropf, J. E.; Currie, K. S. Certain Substituted Amides, Method of Making, and Method of Use Thereof. US Patent Office US 2008/0153834 A1, June 26, 2008; pp 1–47.

(17) Lin, B.; Pease, J. H. A High Throughput Solubility Assay for Drug Discovery Using Microscale Shake-Flask and Rapid UHPLC-UV-CLND Quantification. *J. Pharm. Biomed. Anal.* **2016**, *122*, 126–140.

(18) Dewdney, N. J.; Kondru, R. K.; Lou, Y.; Soth, M. Btk Protein Kinase Inhibitors. US Patent Office US 2009/0105209 A1, April 2009.

(19) Dewdney, N. J.; Lou, Y.; Soth, M. Novel Imidazo[1,2-*a*]Pyridine and Imidazo[1,2-*b*]Pyridazine Derivatives. World Intellectual Property Organization, WO 2009/077334 A1, June 25, 2009; pp 1–118.

(20) Lou, Y.; Han, X.; Kuglstatler, A.; Kondru, R. K.; Sweeney, Z. K.; Soth, M.; McIntosh, J.; Litman, R.; Suh, J.; Kocer, B.; Davis, D.; Park, J.; Frauchiger, S.; Dewdney, N.; Zecic, H.; Taygerly, J. P.; Sarma, K.; Hong, J.; Hill, R. J.; Gabriel, T.; Goldstein, D. M.; Owens, T. D. Structure-Based Drug Design of RN486, a Potent and Selective Bruton's Tyrosine Kinase (BTK) Inhibitor, for the Treatment of Rheumatoid Arthritis. *J. Med. Chem.* **2015**, *58* (1), 512–516.

(21) Barbosa, A.; Blomgren, P. A.; Currie, K. S.; Krishnamoorthy, R.; Kropf, J. E.; Lee, S. H.; Mitchell, S. A.; Ortwine, D. F.; Schmitt, A. C.; Wang, X.; Xu, J.; Young, W.; Zhang, H.; Zhao, Z.; Zhichkin, P. E. Pyridone and Aza-Pyridone Compounds and Methods of Use. World Intellectual Property Organization, WO 2011/140488 A1, November 10, 2011; pp 1–511.

(22) Wuitschik, G.; Carreira, E. M.; Wagner, B.; Fischer, H.; Parrilla, I.; Schuler, F.; Rogers-Evans, M.; Müller, K. Oxetanes in Drug Discovery: Structural and Synthetic Insights. *J. Med. Chem.* **2010**, *53* (8), 3227–3246.

(23) Liu, L.; Di Paolo, J.; Barbosa, J.; Rong, H.; Reif, K.; Wong, H. Antiarthritic Effect of a Novel Bruton's Tyrosine Kinase (BTK) Inhibitor in Rat Collagen-Induced Arthritis and Mechanism-Based Pharmacokinetic/Pharmacodynamic Modeling: Relationships Between Inhibition of BTK Phosphorylation and Efficacy. *J. Pharmacol. Exp. Ther.* **2011**, *338* (1), 154–163.

(24) Katewa, A.; Wang, Y.; Hackney, J. A.; Huang, T.; Suto, E.; Ramamoorthi, N.; Austin, C.; Bremer, M. C.; Chen, J.; Crawford, J. J.; Currie, K. S.; Blomgren, P.; DeVoss, J.; DiPaolo, J. A.; Hau, J.; Johnson, A.; Lee, W. P.; Lesch, J.; DeForge, L.; Lin, Z.; Liimatta, M.; Lubach, J.; McVay, S.; Modrusan, Z.; Nguyen, A.; Wang, J.; Liu, L.; Wong, H.; Young, W. B.; Townsend, M. J.; Reif, K. Specific Inhibition of Btk Blocks Pathogenic Plasma Cell Signatures and Myeloid Cell Associated Kidney Damage in IFN α -Driven Lupus Nephritis. *J. Clin. Invest. Insight* **2017**, *2* (7), e90111.